Fluorescence Resonance Energy Transfer in Calf Thymus DNA from a Long-Lifetime Metal-Ligand Complex to Nile Blue

Jung Sook Kang* and Joseph R. Lakowicz[†]

Department of Oral Biochemistry and Molecular Biology, College of Dentistry and Research Institute for Oral Biotechnology,
Pusan National University, Pusan 602-739, Korea

[†]Center for Fluorescence Spectroscopy, Department of Biochemistry and Molecular Biology, University of Maryland at Baltimore,
Baltimore, MD 21201, USA

We extended the measurable time scale of DNA dynamics to submicrosecond using a long-lifetime metal-ligand complex, $[Ru(phen)_2(dppz)]^{2+}$ (phen =1,10-phenanthroline, dppz = dipyrido[3,2-a:2',3'-c]phenazine) (RuPD), which displays a mean lifetime near 350 ns. We partially characterized the fluorescence resonance energy transfer (FRET) in calf thymus DNA from RuPD to nile blue (NB) using frequency-domain fluorometry with a high-intensity, blue light-emitting diode (LED) as the modulated light source. There was a significant overlap of the emission spectrum of the donor RuPD with the absorption spectrum of the acceptor NB. The Förster distance (R_0) that was calculated from the spectral overlap was 33.4 Å. We observed dramatic decreases in the steady-state fluorescence intensities of RuPD when the NB concentration was increased. The intensity decays of RuPD were matched the closest by a triple exponential decay. The mean decay time of RuPD in the absence of the acceptor NB was 350.7 ns. In a concentration-dependent manner, RuPD showed rapid intensity decay times upon adding NB. The mean decay time decreased to 184.6 ns at 100 μM NB. The FRET efficiency values that are calculated from the mean decay times increased from 0.107 at 20 μM NB to 0.474 at 100 μM NB concentration. The use of FRET with a long-lifetime metal-ligand complex donor is expected to offer the opportunity to increase the information about the structure and dynamics of nucleic acids.

Keywords: Long-lifetime metal-ligand complex, Fluorescence resonance energy transfer, DNA dynamics, Frequency-domain fluorometry, Light-emitting diode.

*To whom correspondence should be addressed.
Tel: 82-51-240-7820; Fax: 82-51-241-1226
E-mail: jsokang@hyowon.pusan.ac.kr

Introduction

Fluorescence resonance energy transfer (FRET) is the transfer of the excited state energy from an initially excited donor to an acceptor (Förster, 1948). The rate of energy transfer depends upon the extent of spectral overlap of the emission spectrum of the donor with the absorption spectrum of the acceptor, the quantum yield of the donor, the relative orientation of the donor and acceptor transition dipoles, and the distance between the donor and acceptor molecules. The distance dependence of FRET resulted in its widespread use as a "spectroscopic ruler" to determine the distance (generally 10-80 Å) between a donor and an acceptor molecule (Steinberg, 1971; Stryer, 1978; Sung and Kim, 2000). However, FRET has been especially used to study protein structures. FRET applications to nucleic acids recently attracted interest because of the advances in automated oligonucleotide synthesis, as well as the convenient site-specific labeling of synthetic oligonucleotides with suitable probes.

There is currently a great deal of interest in the interaction of transition metal-ligand complexes (MLCs) with DNA. This is partly because of the potential of these compounds as novel probes of DNA conformation and dynamics. Long-lifetime MLCs, which display decay times that range from 100 ns to more than 10 μs, have only recently become available (DeGraff and Demas, 1994; Terpetschnig et al., 1997; Lakowicz et al., 2000). They have favorable chemical, photochemical, and photophysical properties. Because of the large Stokes' shift, the MLCs do not self-quench (Terpetschnig et al., 1997; Lakowicz et al., 2000). In addition, the MLCs show good water solubility, as well as high chemical and photochemical stability (Terpetschnig et al., 1997; Lakowicz et al., 2000). Another favorable property of MLCs is their polarized emission, which makes them useful for microsecond dynamics (Terpetschnig et al., 1997; Lakowicz et al., 2000). Finally, the long lifetimes of MLCs

allow the use of gated detection, which can be employed to suppress interfering autofluorescence from biological samples, thus providing increased sensitivity (Haugen and Lytle, 1981). Barton and co-workers (Friedman et al., 1990; Jenkins et al., 1992; Murphy and Barton, 1993) reported that the dipyrido[3,2-a:2',3'-c]phenazine (dppz) complexes of ruthenium appear to be prime candidates for a spectroscopic probe for nucleic acids because of their "molecular light switch" properties for DNA. Since the luminescent enhancement upon DNA binding is $\geq 10^4$, there is essentially no background with the dppz complexes of ruthenium.

We extended the measurable time scale of DNA dynamics to submicrosecond using a dppz complex of ruthenium, $[Ru(phen)_2(dppz)]^{2+}$ (phen = 1,10-phenanthroline) (RuPD), which displays a mean lifetime near 350 ns. To show the usefulness of RuPD for DNA dynamics, we examined the FRET in calf thymus DNA from RuPD to nile blue (NB) using a frequency-domain fluorometry. As a convenient model system, we chose random labeling of calf thymus DNA with RuPD and NB, which are DNA intercalators. For this study we used a high-intensity, blue light-emitting diode (LED) as the modulated light source. With this LED we were able to directly modulate the excitation light up to 100 MHz without the need for an external modulator like a Pockels cell. We were able to obtain very reliable time-resolved intensity decays.

Materials and Methods

Materials Calf thymus DNA was obtained from Sigma (St. Louis, MO, USA). RuPD was synthesized by the method described previously (Malak et al., 1997). NB was from Aldrich (Milwaukee, WI, USA). All of the reagents were used without further purification. Water was deionized with a Milli-Q system. To convert calf thymus DNA into linear fragments that were comparable in length to one persistent length, about a 5 mg/ml solution of calf thymus DNA was sonicated approximately 10 min while submerged in an ice bath. The sonicated DNA solution was centrifuged for 1 hr at 75,000 × g to remove titanium tip particles and undissolved DNA. All of the experiments were undertaken at room temperature in 2 mM Tris-HCl, pH 8.0, that contained 0.1 mM ethylenediaminetetraacetic acid.

Absorption and steady-state fluorescence measurement About 2-5 mM of the stock solutions of RuPD and NB were prepared in dimethylformamide. The DNA concentration was 1 mM base pair while the concentration of RuPD was 2 0μM. The concentrations of DNA and RuPD were determined using molar extinction coefficients of 13,300 $M^{-1}cm^{-1}$ (expressed as base pair) at 260 nm and 21,000 $M^{-1}cm^{-1}$ at 440 nm, respectively. Quantum yield measurements were performed according to the previously established method using 4-dicyanomethylene-2-methyl-6-(p-dimethylaminostyryl)4H-pyran in methanol ($Q = 0.38$) as a reference (Demas and Crosby, 1971). The optical densities of both the sample and reference were kept below 0.05 at the excitation

wavelengths in order to avoid the inner filter effects, and the emission intensities were integrated throughout the whole spectra. Ultraviolet-visible absorption spectra were measured with a Hewlett-Packard 8453 diode array spectrophotometer. Steady-state fluorescence measurements were carried out using a SLM Model 8000 spectrofluorometer (Spectronic Instruments, Inc., Rochester, NY, USA). The excitation wavelength was 440 nm.

Frequency-domain intensity decay measurements Measurements were performed with the instruments described previously (Lakowicz and Maliwal, 1985) and modified with a data acquisition card from ISS, Inc. (Urbana, IL, USA) (Feddersen et al., 1989). The excitation source was a blue LED LNG992CFBW (Panasonic, Japan) with a luminous intensity of 1,500 mcd. A LED driver LDX-3412 (ILX Lightwave, Boseman, MO, USA) provided 30 mA of the current at frequencies from 0.1 to 10 MHz. A 450 ± 20 nm interference filter and a 620 nm cut-off filter were used for isolating the excitation and emission, respectively. Rhodamine B in water ($\tau = 1.68$ ns) was utilized as a lifetime standard.

The intensity decays were recovered from the frequency-domain data in terms of a multiexponential model:

$$I(t) = \sum_{i=1}^{n} \alpha_i e^{-t/\tau_i} \tag{1}$$

where the preexponential factors α_i are the amplitude of each component, $\Sigma \alpha_i = 1.0$, τ_i are the decay times, and n are the numbers of exponential components. These values were determined by a nonlinear least squares analysis, as described previously (Gratton et al., 1984; Lakowicz et al., 1984). Mean lifetimes were calculated by:

$$\langle \tau \rangle = \frac{\sum_i \alpha_i \tau_i^2}{\sum_i \alpha_i \tau_i} = \sum_i f_i \tau_i \tag{2}$$

where f_i is the fractional steady-state contribution of each component to the total emission, and Σf_i is normalized to unity. f_i is given by

$$f_i = \frac{\alpha_i \tau_i}{\sum_j \alpha_j \tau_j} \tag{3}$$

The best fits were obtained by minimizing χ_R^2 values:

$$\chi_R^2 = \frac{1}{\nu} \sum_\omega \left[\left(\frac{\varphi_\omega - \varphi_{c\omega}}{\delta\varphi} \right)^2 + \left(\frac{m_\omega - m_{c\omega}}{\delta m} \right)^2 \right] \tag{4}$$

where ν is the number of degrees of freedom, and φ_ω and m_ω are the experimental phase and modulation, respectively. The subscript c is used to indicate calculated values for the assumed values of α_i and τ_i, and $\delta\varphi$ and δm are the experimental uncertainties. Here, the values of $\delta\varphi$ and δm were set at 0.2° and 0.005, respectively.

Theory for Fluorescence Resonance Energy Transfer

Förster (1948) pioneered the study of FRET. The theory for FRET can be summarized as follows (Lakowicz, 1999). The rate of energy transfer from a donor to an acceptor (k_T) is given by

$$k_T = \frac{1}{\tau_D}\left(\frac{R_0}{r}\right)^6 \qquad (5)$$

where τ_D is the decay time of the donor in the absence of an acceptor, R_0 is the Förster distance, and r is the donor-acceptor distance. The Förster distance R_0 is the distance at which FRET is 50% efficient and given by

$$R_0 = (J(\lambda)\kappa^2 Q_D n^{-4})^{1/6} \times 9.78 \times 10^3 \qquad (6)$$

where $J(\lambda)$ is the spectral overlap integral of the donor emission and acceptor absorption, κ^2 is the orientation factor for the dipole-dipole interaction, Q_D is the quantum yield of the donor in the absence of an acceptor, and n is the refractive index of the medium. The overlap integral $J(\lambda)$ expresses the degree of spectral overlap between the donor emission and the acceptor absorption

$$J(\lambda) = \int_0^\infty F_D(\lambda)\varepsilon_A(\lambda)\lambda^4 d\lambda \qquad (7)$$

where $F_D(\lambda)$ is the corrected fluorescence intensity of the donor in the wavelength range λ to $\lambda + \Delta\lambda$, with the total intensity (area under the curve) normalized to unity, and $\varepsilon_A(\lambda)$ is the extinction coefficient of the acceptor at λ, which is typically in the unit of $M^{-1}cm^{-1}$.

The efficiency of FRET (E) is the fraction of photons that are absorbed by the donor, which are transferred to the acceptor and calculated by

$$E = 1 - \frac{\tau_{DA}}{\tau_D} \qquad (8)$$

where τ_D and τ_{DA} are the mean donor decay times in the absence and presence of the acceptor, respectively.

Results and Discussion

Steady-state spectra In this study, we partially characterized the FRET in calf thymus DNA from a long-lifetime donor RuPD to the long-wavelength acceptor NB. The chemical structures of RuPD and NB are shown in Fig. 1. Fig. 2 shows the absorption and emission spectra of the RuPD-NB donor-acceptor pair. There is a significant overlap of the emission spectrum of the donor RuPD with the absorption spectrum of the acceptor NB. The spectral overlap integral $(J(\lambda))$ was used to calculate the Förster distance R_0 according to Eq. (6). The result is summarized in Table 1. The R_0 value for the RuPD-
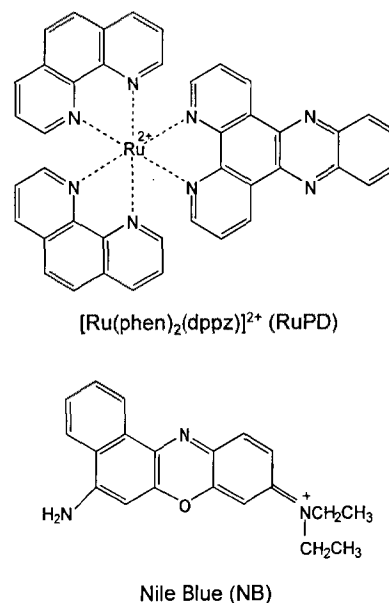

[Ru(phen)₂(dppz)]²⁺ (RuPD)

Nile Blue (NB)

Fig. 1. Chemical structures of [Ru(phen)₂(dppz)]²⁺ (RuPD) and nile blue (NB).
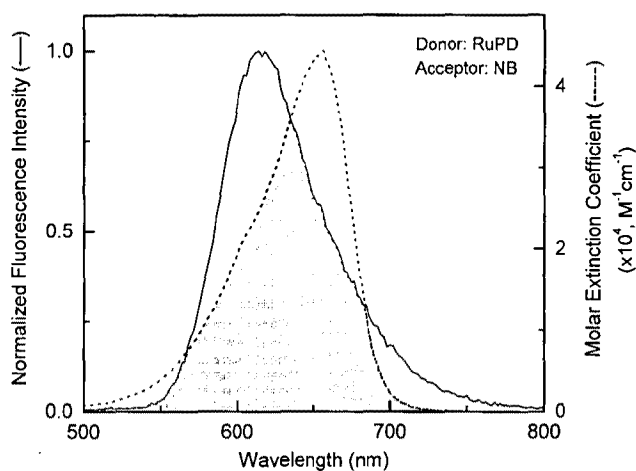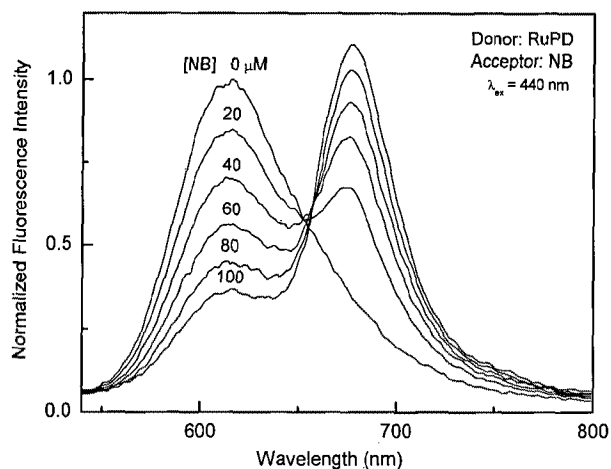

Fig. 2. Emission spectrum (–) of the RuPD-calf thymus DNA complex and absorption spectrum (---) of the NB-calf thymus DNA complex. The spectral overlap shown in gray was used to calculate the Förster distance R_0.

NB pair was 33.4 Å. In the calculation of R_0, the value of κ^2 was 1.25, which was previously used for FRET for a number of DNA-bound fluorophores (Maliwal et al., 1995; Murata et al., 2000). The value of the refractive index (n) was taken as 1.5 (Maliwal et al., 1995; Murata et al., 2000). Fig. 3 shows the emission spectra of RuPD that was intercalated into DNA upon adding the acceptor NB. The steady-state fluorescence intensities of RuPD with a peak at about 616 nm decreased dramatically with an increase in the NB concentration. We observed not only the quenching of the donor RuPD emission but also the enhancement of the acceptor NB emission that was centered at about 676 nm (Fig. 3). However, the

Fig. 3. Emission spectra of the RuPD-calf thymus DNA complex in the absence and presence of different concentrations of NB.

Fig. 4. Frequency-domain intensity decays of the RuPD-calf thymus DNA complex in the absence and presence of different concentrations of NB. The symbols represent the measured phase and modulation values. The solid lines show the best multiexponential fits to the data. The middle and lower panels show plots of the residuals between the experimental data and the fitted curve.

enhancement of the NB emission was much smaller for RuPD than for the other dppz complex of ruthenium, $[Ru(bpy)_2(dppz)]^{2+}$ (bpy = 2,2'-bipyridine) (RuBD) (Lakowicz *et al.*, 2001). We showed that the enhancement of the acceptor emission from FRET is larger for RuBD, a low quantum yield donor ($Q = 0.008$), than for the high quantum yield donors-acridine orange ($Q = 0.392$) and ethidium bromide ($Q = 0.219$) (Lakowicz *et al.*, 2001). Therefore, it seems that the higher quantum yield of RuPD ($Q = 0.017$, Table 1) resulted in a lower enhancement of the acceptor NB emission than RuBD did. This result of a larger enhancement with a lower quantum yield donor can be understood by the theory presented by Lakowicz *et al.* (2001). In the absence of energy transfer, the total fluorescence intensity is given by

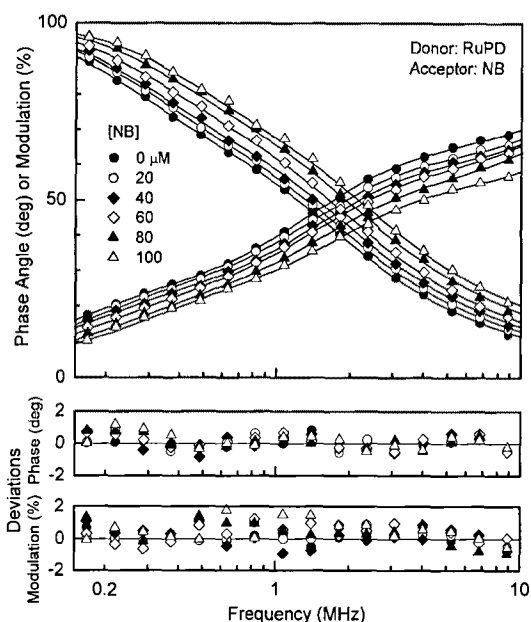$$F_T^o = k(\varepsilon_A Q_A + \varepsilon_D Q_D) \qquad (9)$$

where ε_D and ε_A are the molar extinction coefficients of the donor (ε_D) and acceptor (ε_A) at the excitation wavelength, and Q_D and Q_A are the quantum yields of the donor and acceptor, respectively, and k is a constant that contains the excitation intensity, concentration, and instrumental factors. In the presence of 100% energy transfer, the total intensity is

Table 1. Donor quantum yield (Q_D), spectral overlap integral ($J(\lambda)$) and Förster distance (R_0) of [Ru(phen)_2(dppz)]^{2+}-nile blue donor-acceptor pair in calf thymus DNA

$Q_D{}^a$	$J(\lambda)^b$ $(\times 10^{-13}, M^{-1}cm^3)$	$R_0{}^b$ (Å)
0.017	3.766	33.4

[a]4-Dicyanomethylene-2-methyl-6-(*p*-dimethylaminostyryl)4*H*-pyran in methanol ($Q = 0.38$) was used as a quantum yield reference.
[b]$J(\lambda)$ and R_0 were calculated according to Eqs. (7) and (6), respectively.

$$F_T = k(\varepsilon_A + \varepsilon_D)Q_A = k(\varepsilon_A Q_A + \varepsilon_D Q_A) \qquad (10)$$

Hence, the enhancement of the total emission is given by

$$\frac{F_T}{F_T^o} = \frac{\varepsilon_A Q_A + \varepsilon_D Q_A}{\varepsilon_A Q_A + \varepsilon_D Q_D} \qquad (11)$$

If the acceptor does not absorb at the excitation wavelength ($\varepsilon_A = 0$), the enhancement is then proportional to the ratio Q_A/Q_D.

Time-resolved donor intensity decays To provide further evidence for FRET from RuPD to NB, we carried out frequency-domain intensity decay measurements. Fig. 4 shows the frequency responses of RuPD that is intercalated into DNA upon adding NB. The intensity decays were analyzed in terms of the multiexponential model, according to Eqs. (1)-(4). The results are summarized in Table 2. In the absence of the acceptor, the intensity decay of RuPD was matched the closest by three exponential decays with a mean decay time of 350.7 ns, which is comparable to the values reported previously for calf thymus DNA (Jenkins *et al.*, 1992; Murphy and Barton, 1993; Holmin *et al.*, 1998). To be more specific, the intensity decay of RuPD in the absence of an acceptor is intrinsically multi- or non-exponential. The origin of this heterogeneity is unclear. In the presence of the acceptor, the RuPD intensity decays became more

Table 2. Multiexponential intensity decay analysis

NB Conc. (μM)	τ_i (ns)	α_i	f_i^a	$<\tau>^a$ (ns)	χ_R^{2b}
0	691.2	0.068	0.417	350.7	1.9
	117.5	0.505	0.524		
	15.7	0.427	0.059		
20	614.8	0.066	0.416	313.3	2.9
	110.4	0.449	0.510		
	14.8	0.485	0.074		
40	596.8	0.058	0.399	293.0	4.3
	104.2	0.434	0.517		
	14.5	0.508	0.084		
60	523.0	0.057	0.373	250.1	3.4
	101.9	0.415	0.526		
	15.4	0.528	0.101		
80	450.1	0.054	0.354	209.7	3.6
	92.9	0.381	0.520		
	15.1	0.565	0.126		
100	384.2	0.051	0.375	184.6	4.8
	78.7	0.333	0.497		
	11.0	0.615	0.128		

[a]Fractional intensities f_i and mean lifetimes $<\tau>$ were calculated using Eqs. (3) and (2), respectively.
[b]The χ_R^2 values were calculated by Eq. (4). The standard errors of phase angle and modulation were set at 0.2 degree and 0.005, respectively.

heterogeneous. This effect is due to a range of donor-acceptor distances for the probes that are randomly distributed along the double-helical DNA. The extent of heterogeneity in the donor intensity decay can be recognized by the χ_R^2 values for the three-exponential fit. This value increased from 1.9 in the absence of the acceptor to 4.8 with 100 μM NB (Table 2). However, the intensity decays could still be more complex because it is almost impossible to resolve the intensity decay data into more than three exponential components (Small and Isenberg, 1977). As the acceptor concentration increases, the frequency responses shift to high modulation frequencies, which indicates a decrease in the mean decay time (Fig. 4 and Table 2). The mean decay time decreased to 184.6 ns at 100 μM NB. It is informative to examine the intensity decays in the time-domain that was reconstructed from the frequency-domain data (Fig. 5). The time-domain representation of the multiexponential analysis data clearly shows the presence of a fast component with increasing amplitude as the acceptor NB concentration is increased. Table 3 shows the efficiency of FRET (E). The transfer efficiency can be calculated from either steady-state or time-resolved data. Because lifetimes are independent of fluorophore concentration and other artifacts that affect fluorescence intensity measurements, time-resolved data are much more reliable than steady-state data. So, we calculated the FRET efficiency from the time-resolved data according to Eq. (8). The FRET efficiency values that were
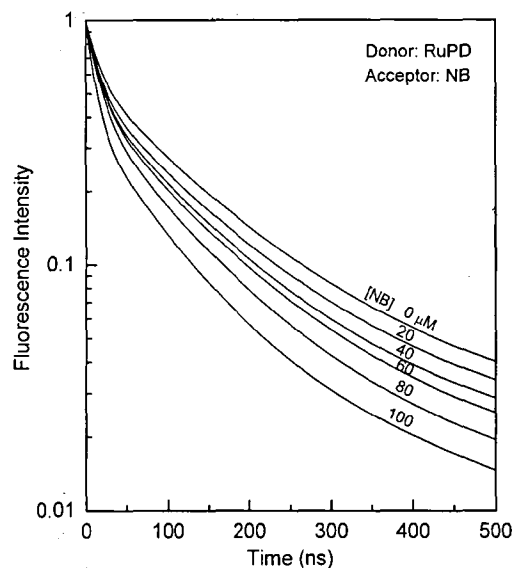
Fig. 5. Time-domain representation of the intensity decays of the RuPD-calf thymus DNA complex in the absence and presence of different concentrations of NB.

Table 3. The FRET efficiency (E)

NB Concentration (μM)	E^a
20	0.107
40	0.165
60	0.2 87
80	0.402
100	0.474

[a]The FRET efficiency values were calculated according to Eq. (8).

calculated from the mean decay times increased from 0.107 at 20 μM NB to 0.474 at 100 μM NB concentration.

The use of FRET with a long-lifetime MLC donor as a novel method for studying DNA structure and dynamics

Although other methods, such as nucleic magnetic resonance (Jung et al., 1999; Cho et al., 2000; Lee and Choi, 2000) and X-ray diffraction (Lilley, 2000) methods, can be useful for distance determination, FRET is the only method that provides information about the changes in the distance in the process of conformational changes of biomolecules, both in the solution and in living organisms in vivo (Lankiewicz et al., 1997). FRET has already provided considerable information about the solution structure of three- (Yang and Millar, 1996) and four-way (Eis and Millar, 1993; Clegg et al., 1994) DNA junctions, curved DNA (Tóth et al., 1998), and the kinking of DNA helices by bulged nucleotides (Gohlke et al., 1994). FRET has also been employed to determine helical handedness of double-stranded DNA in solution (Jares-Erijman and Jovin, 1996), as well as to measure distances and distance-distributions along the helix backbone in dye-linked

DNA (Hochstrasser et al., 1992; Maliwal et al., 1995; Murata et al., 2000). Other FRET studies investigated DNA hybridization (Masuko et al., 2000), DNA triple helix formation (Mergny et al., 1994; Scaria et al., 1995), DNA-protein complexes (Hill and Royer, 1997), and the kinetics of enzyme-catalyzed DNA cleavage (Ghosh et al., 1994). However, the short decay times of about 1 to 20 ns that are encountered in most of the studies of FRET have been a serious limitation of the use of time-resolved FRET for DNA structure and dynamics, since DNA is expected to display a wide range of relaxation times (Allison and Schurr, 1979; Barkley and Zimm, 1979). Only the nanosecond motions can be effectively probed with the nanosecond-lifetime probes.

The use of long-lifetime MLCs to measure DNA dynamics is just beginning (Malak et al., 1997; Terpetschnig et al., 1997; Lakowicz et al., 1995, 2000). Because the interaction of water with the nitrogen atoms on the dppz quenches the luminescence, both RuPD and RuBD display no detectable luminescence in the aqueous solution, but they luminesce brightly in the presence of double-helical DNA. However, the phen derivative RuPD has some advantages over the other bpy derivative RuBD. The lifetimes of RuBD that are bound to calf thymus DNA are about 100 ns (Jenkins et al., 1992; Murphy and Barton, 1993; Lakowicz et al., 1995, 2001; Malak et al., 1997). RuPD showed still longer lifetimes when bound to DNA with a mean decay time of 350.7 ns (Table 2). Also, the quantum yield of RuPD ($Q = 0.017$, Table 1) is more than twice that of RuBD ($Q = 0.008$) (Lakowicz et al., 2001). Because of a longer lifetime and higher quantum yield than the bpy derivative, RuPD is expected to have a number of applications in studies of nucleic acid structure and dynamics. We believe that the use of FRET with a long-lifetime MLC donor could increase opportunities for information about the structure and dynamics of nucleic acids.

Donor-acceptor diffusion increases the efficiency of energy transfer between covalently linked donor-acceptor pairs (Lakowicz et al., 1994) and in the homogenous solution (Steinberg and Katchalski, 1968). For the lifetimes of 1-20 ns that are displayed by most DNA fluorophores, there is little translational displacement during the lifetime of the donor. However, diffusion-enhanced FRET was demonstrated in millisecond-lifetime lanthanide complexes (Stryer et al., 1982). Thus, it is possible that the FRET efficiency was somewhat enhanced by diffusive processes in DNA during the long decay time of RuPD ($<\tau> = 350.7$ ns, Table 2). In particular, RuPD dissociates from DNA and reassociates at different locations. Further experimentation is required to determine if the hopping of RuPD along DNA occurs on the submicrosecond time scale. In the absence of diffusion, Blumen and Manz (1979) derived an equation for the ensemble averaged time decay of an excited donor in the presence of randomly distributed acceptors in one dimension in a lattice structure. Once we derive a proper mathematical model that incorporates diffusion to the one-dimensional FRET model of Blumen and Manz (1979), we will be able to fully characterize the FRET in calf thymus DNA from RuPD, a long-lifetime MLC donor to the NB acceptor.

The use of LEDs as the source of excitation An important point of this study was our use of a high-intensity, blue LED as the source of excitation. We were able to obtain approximately 3 to 5 mW of excitation power, depending on the LED current. Since its first introduction in 1995, a variety of LEDs (such as the high intensity ultraviolet, blue, and green GaN LEDs) have been developed as an inexpensive and convenient light source. The use of the LED also allowed us a simpler "turn-key" operation-i.e., less optical adjustments and easier electronic operations. Direct electronic modulation of up to 100 MHz eliminates the expensive and cumbersome electro-optic modulators that are found in most frequency-domain instruments (Sipior et al., 1996). We expect that the low cost of LEDs, together with its simpler mode of operation, will allow laboratories to perform time-resolved fluorescence measurements for a wide variety of applications.

References

Allison, S. A. and Schurr, J. M. (1979) Torsion dynamics and depolarization of fluorescence of linear macromolecules. 1. Theory and application to DNA. *Chem. Phys.* **41**, 35-59.

Barkley, M. D. and Zimm, B. H. (1979) Theory of twisting and bending of chain macromolecules; analysis of the fluorescence depolarization of DNA. *J. Chem. Phys.* **70**, 2991-3007.

Blumen, A. and Manz, J. (1979) On the concentration and time dependence of the energy transfer to randomly distributed acceptors. *J. Chem. Phys.* **71**, 4694-4702.

Cho, Y. S., Chang, S.-G., Choi, K.-D., Shin, H. C., Ahn, B. Y. and Kim, K.-S. (2000) Solution structure of an active mini-proinsulin, M2PI: inter-chain flexibility is crucial for insulin activity. *J. Biochem. Mol. Biol.* **33**, 120-125.

Clegg, R. M., Murchie, A. I. H. and Lilley, D. M. J. (1994) The solution structures of the four-way DNA junction at low-salt conditions: a fluorescence resonance energy transfer analysis. *Biophys. J.* **66**, 99-109.

DeGraff, B. A. and Demas, J. N. (1994) Direct measurement of rotational correlation times of luminescent ruthenium(II) molecular probes by differential polarized phase fluorometry. *J. Phys. Chem.* **98**, 12478-12480.

Demas, J. N. and Crosby, G. A. (1971) The measurement of photoluminescence quantum yields. A review. *J. Phys. Chem.* **75**, 991-1024.

Eis, P. S. and Millar, D. P. (1993) Conformational distributions of a four-way DNA junction revealed by time-resolved fluorescence energy transfer. *Biochemistry* **32**, 13852-13860.

Feddersen, B. A., Piston, D. W. and Gratton, E. (1989) Digital parallel acquisition in frequency domain fluorimetry. *Rev. Sci. Instrum.* **60**, 2929-2936.

Förster, Th. (1948) Intermolecular energy migration and fluorescence. *Ann. Phys.* **2**, 55-75. Translated by Knox R. S., Department of Physics and Astronomy, University of Rochester, Rochester, NY 14627.

Friedman, A. E., Chambron, J.-C., Sauvage, J.-P., Turro, N. J. and Barton, J. K. (1990) Molecular "light switch" for DNA: Ru(bpy)$_2$(dppz)$^{2+}$. *J. Am. Chem. Soc.* **112**, 4960-4962.

Ghosh, S. S., Eis, P. S., Blumeyer, K., Fearon, K. and Millar, D. P. (1994) Real time kinetics of restriction endonuclease cleavage monitored by fluorescence resonance energy transfer. *Nucleic Acids Res.* **22**, 3155-3159.

Gohlke, C., Murchie, A. I. H., Lilley, D. M. and Clegg, R. M. (1994) Kinking of DNA and RNA helices by bulged nucleotides observed by fluorescence resonance energy transfer. *Proc. Natl. Acad. Sci. USA* **91**, 11660-11664.

Gratton, E., Lakowicz, J. R., Maliwal, B. P., Cherek, H. and Laczko, G. (1984) Resolution of mixtures of fluorophores using variable-frequency phase and modulation data. *Biophys. J.* **46**, 478-486.

Haugen, G. R. and Lytle, F. E. (1981) Quantitation of fluorophores in solution by pulsed laser excitation and time-filtered detection. *Anal. Chem.* **53**, 1554-1559.

Hill, J. J. and Royer, C. A. (1997) Fluorescence approaches to study of protein-nucleic acid complexation. *Methods Enzymol.* **278**, 390-416.

Hochstrasser, R. A., Chen, S.-M. and Millar, D. P. (1992) Distance distribution in a dye-linked oligonucleotide determined by time-resolved fluorescence energy transfer. *Biophys. Chem.* **45**, 133-141.

Holmin, R. E., Stemp, E. D. A. and Barton, J. K. (1998) Ru(phen)$_2$dppz$^+$ luminescence: dependence on DNA sequences and groove-binding agents. *Inorg. Chem.*, **37**, 29-34.

Jares-Erijman, E. A. and Jovin, T. M. (1996) Determination of DNA helical handedness by fluorescence resonance energy transfer. *J. Mol. Biol.* **257**, 597-617.

Jenkins, Y., Friedman, A. E., Turro, N. J. and Barton, J. K. (1992) Characterization of dipyridophenazine complexes of ruthenium(II): The light switch effect as a function of nucleic acid sequence and conformation. *Biochemistry* **31**, 10809-10816.

Jung, J.-W., An, J. H., Kim, Y. S., Bang, E.-J. and Lee, W. (1999) Determination of the solution structure of malonyl-CoA by two-dimensional nuclear magnetic resonance spectroscopy and dynamical simulated annealing calculations. *J. Biochem. Mol. Biol.* **32**, 288-293.

Lakowicz, J. R. (1999) *Principles of Fluorescence Spectroscopy*, 2nd ed., pp. 368-374, Kluwer Academic/Plenum Publishers, New York.

Lakowicz, J. R., Gratton, E., Laczko, G., Cherek, H. and Limkeman, M. (1984) Analysis of fluorescence decay kinetics from variable-frequency phase shift and modulation data. *Biophys. J.* **46**, 463-477.

Lakowicz, J. R., Gryczynski, I., Kúsba, J., Wiczk, W., Szmacinski, H. and Johnson, M. L. (1994) Site-to-site diffusion in proteins as observed by energy transfer and frequency domain fluorometry. *Photochem. Photobiol.* **59**, 16-29.

Lakowicz, J. R., Gryczynski, I., Piszczek, G., Tolosa, L., Nair, R., Johnson, M. L. and Nowaczyk, K. (2000) Microsecond dynamics of biological macromolecules. *Methods Enzymol.* **323**, 473-509.

Lakowicz, J. R., Malak, H, Gryczynski, I., Castellano, F. N. and Meyer, G. J. (1995) DNA dynamics observed with long lifetime metal-ligand complexes. *Biospectroscopy* **1**, 163-168.

Lakowicz, J. R. and Maliwal, B. P. (1985) Construction and performance of a variable-frequency phase-modulation fluorometer. *Biophys. Chem.* **21**, 61-78.

Lakowicz, J. R., Piszczek, G. and Kang, J. S. (2001) On the possibility of long-wavelength long-lifetime high-quantum yield luminophores. *Anal. Biochem.* **288**, 62-75.

Lankiewicz, L., Malicka, J. and Wiczk, W. (1997) Fluorescence resonance energy transfer in studies of interchromophoric distances in biomolecules. *Acta Biochim. Pol.* **44**, 477-489.

Lee, J.-H. and Choi, B.-S. (2000) Structure of a DNA duplex containing a site-specific Dewar isomer: structural influence of the 3'-T · G base pair of the Dewar product. *J. Biochem. Mol. Biol.* **33**, 268-275.

Lilly, D. M. (2000) Structures of helical junctions in nucleic acids. *Q. Rev. Biophys.* **33**, 109-159.

Malak, H., Gryczynski, I., Lakowicz, J. R., Meyers, G. J. and Castellano, F. N. (1997) Long-lifetime metal-ligand complexes as luminescent probes for DNA. *J. Fluorescence* **7**, 107-112.

Maliwal, B. P., Kúsba, J. and Lakowicz, J. R. (1995) Fluorescence energy transfer in one dimension: frequency-domain fluorescence study of DNA-fluorophore complexes. *Biopolymers* **35**, 245-255.

Masuko, M, Ohuchi, S., Sode, K., Ohtani, H. and Shimadzu, A. (2000) Fluorescence resonance energy transfer from pyrene to perylene labels for nucleic acid hybridization assays under homogeneous solution conditions. *Nucleic Acids Res.* **28**, e34 (i-viii).

Mergny, J.-L., Garestier, T., Rougée, M., Lebedev, A. V., Chassignol, M., Thuong, N. T. and Hélène, C. (1994) Fluorescence energy transfer between two triple helix-forming oligonucleotides bound to duplex DNA. *Biochemistry* **33**, 15321-15328.

Murata, S.-I., Kúsba, J., Piszczek, G., Gryczynski, I. and Lakowicz, J. R. (2000) Donor fluorescence decay analysis for energy transfer in double-helical DNA with various acceptor concentrations. *Biopolymers* **57**, 306-315.

Murphy, C. J. and Barton, J. K. (1993) Ruthenium complexes as luminescent reporters of DNA. *Methods Enzymol.* **226**, 576-594.

Scaria, P. V., Will, S., Levenson, W. C. and Shafer, R. H. (1995) Physicochemical studies of the d(G3T4G3)*d(G3A4G3).d(C3T4C3) triple helix. *J. Biol. Chem.* **270**, 7295-7303.

Sipior, J., Carter, J. M., Lakowicz, J. R. and Rao, G. (1996) Single quantum well light-emitting diodes demonstrated as excitation sources for nanosecond phase modulation fluorescence lifetime measurements. *Rev. Sci. Instr.* **67**, 3795-3798.

Small, E. W. and Isenberg, I. (1977) Hydrodynamic properties of a rigid molecule: Rotational and linear diffusion and fluorescence anisotropy. *Biopolymers* **16**, 1907-1928.

Steinberg, I. Z. (1971) Long-range nonradiative transfer of electronic excitation energy in proteins and polypeptides. *Annu. Rev. Biochem.* **40**, 83-114.

Steinberg, I. Z. and Katchalski, E. (1968) Theoretical analysis of the role of diffusion in chemical reactions, fluorescence quenching, and nonradiative energy transfer. *J. Chem. Phys.* **48**, 2404-2410.

Stryer, L. (1978) Fluorescence energy transfer as a spectroscopic ruler. *Annu. Rev. Biochem.* **47**, 819-846.

Stryer, L., Thomas, D. D., and Meares, C. F. (1982) Diffusion-enhanced fluorescence energy transfer. *Ann. Rev. Biophys. Bioeng.* **11**, 203-222.

Sung, B. K. and Kim, Y. T. (2000) Structural arrangement for functional requirements of brain recombinant 4-aminobutyrate aminotransferase. *J. Biochem. Mol. Biol.* **33**, 43-48.

Terpetschnig, E., Szmacinski, H. and Lakowicz, J. R. (1997)

Long-lifetime metal-ligand complexes as probes in biophysics and clinical chemistry. *Methods Enzymol.* **278**, 295-321.

Tóth, K., Sauermann, V. and Langowski, J. (1998) DNA curvature in solution measured by fluorescence resonance energy transfer. *Biochemistry* **37**, 8173- 8179.

Yang, M. and Millar, D. P. (1996) Conformational flexibility of three-way DNA junctions containing unpaired nucleotides. *Biochemistry* **35**, 7959-7967.